Understanding the patterns of biological response to physical forcing in the Alborán Sea (western Mediterranean)

Gabriel Navarro,[1] Águeda Vázquez,[2] Diego Macías,[1] Miguel Bruno,[3] and Javier Ruiz[1]

Received 20 September 2011; revised 29 October 2011; accepted 1 November 2011; published 9 December 2011.

[1] A singular value decomposition (SVD) analysis was performed to determine the coupled modes of variability of satellite surface chlorophyll (CHL) and absolute dynamic topography (ADT) data for the Alborán Sea (western Mediterranean) during a 12-year period (1998–2009). From this analysis we have been able to detect features of the Alborán Sea dynamics that had not been recognized in previous research on the primary production of this basin. We have found that the two leading SVD modes represent more than 97% of the total squared covariance. The first mode is associated with the inverse barometer and its impact on chlorophyll distribution, whereas the second physical mode can explain the distribution of eutrophic and oligotrophic waters in the Alborán Sea. The results also confirm that the phytoplankton in the basin is very tightly controlled by meteorological and physical processes, via the advection of properties through the Strait, by the influence of Atlantic Jet intensity, which controls the gyres of the basin, and by the activation of up- or down-welling coastal processes by wind. **Citation:** Navarro, G., Á. Vázquez, D. Macías, M. Bruno, and J. Ruiz (2011), Understanding the patterns of biological response to physical forcing in the Alborán Sea (western Mediterranean), *Geophys. Res. Lett.*, *38*, L23606, doi:10.1029/2011GL049708.

1. Introduction

[2] The Alborán Sea (Figure 1) connects the Mediterranean Sea with the Atlantic Ocean through the Strait of Gibraltar. It is a highly dynamic and biologically productive region mainly forced by the Atlantic Jet (AJ) moving through the Strait. In recent years, several studies have described the physical and biological coupling in this area, using in-situ data [e.g., *Macías et al.*, 2006], modeling [*Macías et al.*, 2007a] and remote sensing associated with sea surface temperature [e.g., *Parada and Canton*, 1998], altimetry data [*Larnicol et al.*, 2002; *Snaith et al.*, 2003; *Isern-Fontanet et al.*, 2006; *Pascual et al.*, 2007; *Jordi and Wang.*, 2009] and ocean color images [*García-Gorriz and Carr*, 1999; *Macías et al.*, 2007b; *Vázquez et al.*, 2009].

[3] In addition, *Macías et al.* [2008] have established the relationship between meteorological forcing and the distribution of biogeochemical variables in the north-western Alborán Sea. During a westerly wind regime, lower sea level pressure (SLP) in the Mediterranean enhances the inflow of the Atlantic waters through the Strait, increasing the AJ velocity and displacing the jet towards the Spanish coast. This reinforces the coastal upwelling and, therefore, increases the nearshore chlorophyll concentration. Higher SLP in the Mediterranean (associated with easterly winds in this region), diminish the inflow of Atlantic waters, decrease the jet velocity and cause its southward displacement [*García-Lafuente et al.*, 1998], which diminishes the coastal upwelling [*Macías et al.*, 2008]. Moreover, *Vázquez et al.* [2009] have described how chlorophyll-rich coastal waters are transported to the main channel of the Strait (at the Camarinal Sill, CS) during the generation of internal waves [*Macías et al.*, 2010; *Bartual et al.*, 2011], and how the chlorophyll patches associated with the front of the internal waves travel into the Alborán Sea [*Macías et al.*, 2006].

[4] The availability of satellite imagery of hydrodynamic and biological variables for the same period has allowed us to investigate the main temporal and spatial patterns of covariability between ocean surface chlorophyll (CHL) and absolute dynamical topography (ADT) in the Alborán Sea. Since the Mediterranean Sea is nutrient-limited, its biological production is closely coupled to the physical processes that provide nutrients to the surface [*Jordi et al.*, 2009]. In this context, we have studied the relationships between meteorological and hydrodynamical processes and the modes of variability of surface CHL distribution as a proxy for phytoplankton biomass. For this purpose, we have performed a Singular Value Decomposition (SVD) analysis [*Prohaska*, 1976; *Wallace et al.*, 1992; *Bretherton et al.*, 1992] of remotely-sensed estimates of CHL together with simultaneous altimetry satellite data for the 12-year period (1998–2009). To make the research more comprehensive, SLP data for the western Mediterranean have been included in the analysis to study the relationship between meteorology, hydrodynamics and plankton distribution.

2. Material and Methods

2.1. Ocean Color Data

[5] Ocean surface CHL data were downloaded from the GlobColour Project (http://www.globcolour.info/) which produces global ocean color maps (Level-3) by merging the data from the three sensors SeaWiFS, MODIS and MERIS, for the period between January 1998 and December 2009. With these data sets, cloud cover is reduced and, therefore, more useful images become available. Spatial and temporal resolutions of these composite images are 4 km and 8 days respectively. The Region of Interest (ROI) is located in the western Mediterranean, at the western end of the Alborán Sea (35°–37°N and 6° 12′–2° 30′ W). A set of 552 8-day

[1]Departamento de Ecología y Gestión Costera, Instituto de Ciencias Marinas de Andalucía, CSIC, Puerto Real, Spain.
[2]Departamento de Física Aplicada, Universidad de Cádiz, Puerto Real, Spain.
[3]Centro Andaluz de Ciencia y Tecnología Marinas, Universidad de Cádiz, Puerto Real, Spain.

0094-8276/11/2011GL049708

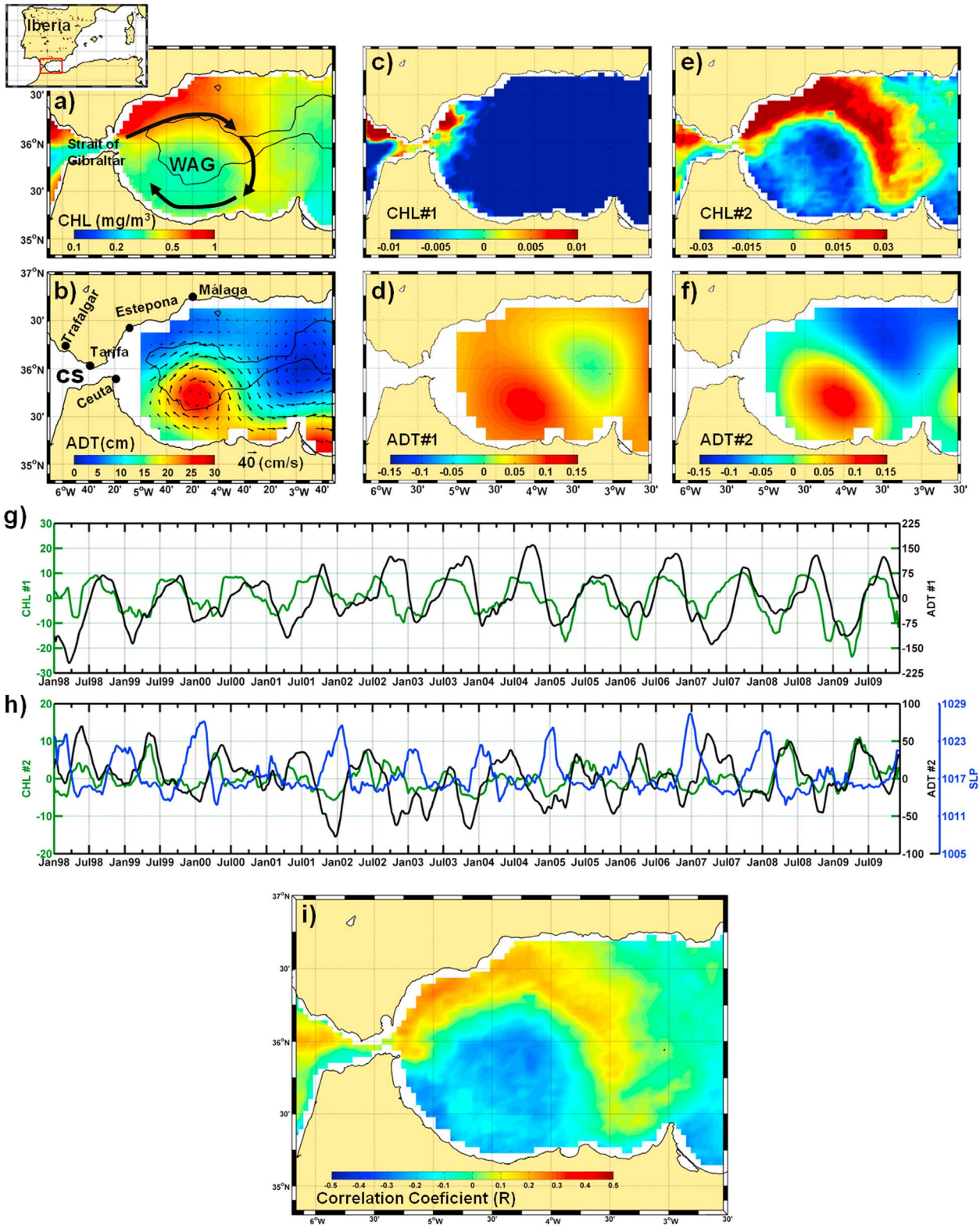

Figure 1. (a) Climatological distribution of CHL (in mg/m^3) over the period 1998 to 2009. The black line indicates the 1000 m isobath. WAG is the West Alboran Gyre (schematically after *Arnone et al.* [1990]). (b) Climatological pattern of ADT (in cm) and associated geostrophic currents during the same period. Spatial patterns of (c) CHL#1, (d) ADT#1, (e) CHL#2 and (f) ADT#2 for the first two SVD modes. (g) Time series of expansion coefficients (CHL green line and ADT black line) of the first SVD mode. (h) Time series of expansion coefficients (CHL green line and ADT black line) of the second SVD and SLP (blue line, in mb). (i) Heterogeneous map between the time series of the expansion coefficient of ADT (SVD # 2) and the CHL field over the Alborán Sea. Time series are smoothed by a three-bin running boxcar averaging to dampen high frequency.

composite images have been used to performed the SVD analysis. For a successful application of the SVD analysis methods described below, the pixels with gaps in the CHL composite images are filled using the mean of a 3 × 3 box of surrounding pixels. As a final step before applying the statistical analysis, the remaining spatial gaps are filled by including the temporal means of each pixel. Before performing the SVD, temporal means for each pixel were subtracted [*Björnsson and Venegas*, 1997].

2.2. Altimetry Data

[6] The Absolute Dynamic Topography (ADT) data are delayed-time (dt) gridded and merged products with spatial resolution of 1/8° and temporal resolution of one day. These data were provided by AVISO (http://www.aviso.oceanobs.com) covering the entire Mediterranean Sea and combine information from different missions, which significantly improves the estimation of mesoscale signals [*Le Traon and Dibarboure*, 1999; *Le Traon et al.*, 2001]. To achieve consistency with the temporal resolution of CHL data (8 days), we have averaged eight daily ADT images for the same time period as the CHL composite (8 days). A total of 552 gridded ADT data sets, running from January 1998 to December 2009, was obtained. As with CHL, before performing the SVD, temporal means for each pixel were subtracted [*Björnsson and Venegas*, 1997].

2.3. Sea Level Pressure Data

[7] Sea level pressure data for the western Mediterranean Sea (35°–40° N and 5° W–5° E) were downloaded from the NCEP (http://www.esrl.noaa.gov/psd/) data base. The original daily data (NCEP/NCAR Reanalysis 1 [*Kalnay et al.*, 1996]) were averaged over the same period as the CHL composite (8 days) between January 1998 and December 2009, to match the CHL and ADT time series.

2.4. Singular Value Decomposition

[8] To investigate the combined spatial and temporal covariability between chlorophyll (CHL) and absolute dynamic topography (ADT) data, a SVD technique was employed. The SVD was performed on the cross-covariance matrix between the un-normalized values of each field (CHL anomalies and ADT anomalies) to identify pairs of coupled spatial patterns and their temporal variation, with each pair explaining a fraction of the covariance between the two fields [*Bretherton et al.*, 1992; *Wallace et al.*, 1992; *Björnsson and Venegas*, 1997]. The methodology used in this study is described by *Bretherton et al.* [1992] and *Björnsson and Venegas* [1997]. The results of this analysis produce both a right and a left spatial pattern, and distinct time series for each one. Each leading pair of spatial patterns represents the maximum covariance between the CHL and ADT, and successively smaller fractions of covariance as the singular value decreases [*Bartolacci and Luther*, 1999]. The Squared Covariance Fraction (SCF) represents the magnitude of covariance explained by an individual pair of singular vectors [*Bretherton et al.*, 1992] and was calculated following *Björnsson and Venegas* [1997].

[9] The heterogeneous correlation map was created by calculating correlation coefficient vectors between the second expansion coefficients of the ADT and the CHL values at each grid point. This map indicates how well the grid points in one field can be predicted from the expansion coefficient derived from the other field [*Björnsson and Venegas*, 1997]. This map is produced by plotting *R* (the correlation coefficient) between the time-series of a given mode and the original data of the opposite field. For this study, these heterogeneous maps can be particularly important for observing how the chlorophyll field varies with respect to the seasonality of the physical forcing in the form of ADT.

3. Results

[10] Figures 1a and 1b display the averaged fields (between 1998 and 2009) for CHL and ADT in the Alborán Sea. The highest levels of CHL (Figure 1a) were located on the northern limit of the West Alboran Gyre (WAG), in a coastal band north of CS and on the Moroccan coast of the Gulf of Cádiz, whereas the lowest CHL concentration were found in the centre of the WAG, within the Strait of Gibraltar and in the eastern part of the Alborán Sea. These patterns have been described and analyzed in previous studies [*García-Gorriz and Carr*, 1999; *Baldacci et al.*, 2001; *Navarro and Ruiz*, 2006; *Macías et al.*, 2007b]. ADT climatology (Figure 1b) shows the typical hydrodynamical field in the area, with the WAG described in many studies [e.g., *Arnone et al.*, 1990; *Millot*, 1999].

[11] The two leading SVD modes of coupled CHL and ADT variations account for 97.1% of the total square variance (SCF). The first SVD mode accounts for 87.7% of the SCF. The spatial patterns of this first CHL mode (Figure 1c) show maxima within the Strait and on its north coastline running both west and east from Gibraltar. The maxima are reached during late summer and autumn (Figure 1g). The spatial patterns of the first ADT mode (Figure 1d) present positive values in the whole basin and maximum temporal values during autumn (Figure 1g). A spectral analysis of the expansion coefficient reveals an annual signal in the CHL time series and annual and semiannual signals in the ADT time series (Figure S1 in the auxiliary material).[1] The correlation coefficient between the expansion coefficients of the SVD#1 (CHL vs ADT) is very high for this type of analysis ($R = 0.46$, $p < 0.01$); this suggests a tight coupling between hydrodynamics and phytoplankton abundance (Table S1).

[12] The second SVD mode represents 9.4% of the SCF. The spatial pattern of this second CHL mode (Figure 1e) show very sharp gradients on the northern limits of the WAG, where the AJ is usually located. In the central and northern parts of the AJ, the mode shows positive values whereas it quickly shifts to negative in the south. However, the ADT mode (Figure 1f) displays positive values in the WAG and negative values in the northern part of the basin. The spectral analysis on the expansion coefficient reveals an annual and a semiannual signal in the CHL and ADT time series (Figure S1). The annual maxima in the CHL time series (Figure 1h) occurs in late-winter and early-spring. The correlation between the expansion coefficients of the SVD#2 (CHL vs ADT) is higher ($R = 0.64$, $p < 0.01$) than that calculated for SVD#1; this reflects an even stronger coupling between physics and biology in the dynamics of the second mode (Table S1). The correlation coefficients between CHL#1 vs ADT#2 and CHL#2 vs ADT#1 are 0.03 and

[1] Auxiliary materials are available in the HTML. doi:10.1029/2011GL049708.

−0.03 respectively, not statistically significant in either case ($p > 0.5$, Table S1).

4. Discussion

[13] Using SVD analysis has enabled a study of the covariance between hydrodynamics and phytoplankton distribution in the western Mediterranean. The entirely positive map of the first ADT mode (Figure 1d) indicates that its value rises or descends synchronously in the whole basin. This dynamic suggests a connection with atmospheric pressure forcing, through the inverse barometer response of sea level. Although a significant fraction of the sea level variability is caused by steric effect, sea level in the Mediterranean also is highly variable related to the multiple forces driving the Mediterranean circulation [e.g., *Vigo et al.*, 2005; *Criado-Aldeanueva et al.*, 2008]. The high degree of coherence between SLP and the first mode in the cross-spectral analysis (Figure S1) supports that idea. Note also that, for both SLP and the first temporal mode, most of their variance is located in the same frequency ranges (Figure S1).

[14] The impact on chlorophyll distribution of this physical process is captured by the first CHL mode. A reduction of SLP causes the sea level to rise in the Alborán Sea and, therefore, creates a demand for water that increases the transport by the AJ to levels above its mean value. The reverse holds when SLP increases. During low SLP events, the enhanced eastward transport can advect more chlorophyll from the Gulf of Cádiz into the Mediterranean through the Strait than during mean SLP conditions.

[15] The Trafalgar shallows, east of the Strait, are very productive waters owing to the tidal mixing of the water column [*García-Lafuente and Ruiz*, 2007]. Tidal current also creates large-amplitude internal waves over the Camarinal Sill which are able to transport chlorophyll-enriched coastal waters toward the central zone of the Strait [*Vázquez et al.*, 2009; *Macías et al.*, 2010; *Bartual et al.*, 2011]. The frequent nature of this process (1 or 2 events a day) [*Vázquez et al.*, 2008] facilitates the eastward advection of chlorophyll from the Atlantic to the Mediterranean. This hypothesis of chlorophyll transport is also reinforced by the temporal coincidence between the maxima of the first CHL mode and the reported phytoplankton evolution in the Trafalgar area [*Navarro and Ruiz*, 2006].

[16] It is important to notice that this chlorophyll dynamic was not identified in a previous (individual) CHL SVD analysis of the basin [*Macías et al*., 2007b]. The reason is that, in our coupled analysis, the first mode is assigned to the mode that explains the major part of the covariance (between ADT and CHL variables) while in the *Macías et al.* [2007b] work it was assigned to the mode that explained the major part of the CHL variance alone. Our first mode explains, in connection with the inverse barometer response, as much as 5% of the CHL variance in the region where CHL concentration shows the greatest variability (see Figure S2). The work by *Macías et al.* [2007b] did not include the coupled analysis of CHL and ADT covariance through SVD. Without this coupled analysis, the response of phytoplankton to the inverse barometer effect is masked by the high variance of chlorophyll at the north western Alborán Sea. Therefore, only the joint physical and biological SVD analysis has provided clear evidence of this process affecting chlorophyll distribution in the Strait of Gibraltar and its nearby areas.

[17] The tight control of physical factors over the biology of the Alborán Sea is also evident when analyzing the characteristic features of the second mode. The heterogeneous map shows areas with very high correlation coefficients between the second expansion coefficients of the ADT and the CHL values (Figure 1i). These areas correspond to the regions with the highest and lowest chlorophyll concentrations in the climatological map of the basin (Figure 1a). Therefore, the distribution of eutrophic and oligotrophic waters in the Alborán Sea can be satisfactorily explained by the physical processes forcing the basin dynamics. CHL highs only happen under SLP lows, resulting in a strong negative correlation between the SLP and the expansion coefficients of the second mode (SLP vs CHL#2 $R = -0.54$, $p < 0.01$; SLP vs ADT#2, $R = -0.45$, $p < 0.01$, Table S1). This correlation is also supported by the results of cross-spectral analysis, which yields significant coherence values for both pair of series in the frequency band where they locate their maximum variance (Figure S1).

[18] A decrease in SLP over the western Mediterranean besides reinforcing the AJ, also favors westerly winds in the Alborán Sea [*Macías et al.*, 2008]. Both processes strengthen the anticyclonic circulation of the WAG. In addition, westerly winds activate the coastal upwelling in the north western Alborán Sea [*García-Gorriz and Carr*, 1999]. When the SLP rises, easterlies are favored and the Ekman transport piles up water near the northern coast. The sea level falls in the zone occupied by the WAG and the subinertial flows weaken the AJ [*García-Lafuente et al.*, 1998; *Macías et al.*, 2008]. These physical processes involve downwelling and decreasing cyclonic circulation in the northwest, with a subsequent reduction of primary production in this area.

[19] In conclusion, the coupled SVD analysis of CHL and ADT has detected dynamical features of the Alborán Sea that had not been recognized in previous research on the primary production of this basin. Besides confirming the tight control exerted by physical processes on the phytoplankton distribution of the region, this technique has evidenced the importance of chlorophyll advection through the Strait. This advection implies that a significant portion of the chlorophyll detected by satellites at the western Alborán Sea was produced in the Gulf of Cádiz and transported eastward to the Mediterranean through the Strait of Gibraltar.

[20] **Acknowledgments.** The CHL data were provided by the GlobColour Project (http://www.globcolour.info/) and the ADT products were produced by SSALTO/DUACS and distributed by AVISO (http://www.aviso.oceanobs.com). SLP data were obtained from NCEP Reanalysis data provided by the NOAA/OAR/ESRL PSD, Boulder, Colorado, USA, from their Web site at http://www.esrl.noaa.gov/psd/. This work was supported by research projects P09-RNM-4853, CTM2008-05680-C02-01/MAR, SESAME (FP6-036949), MedEX (CTM2008-04036-E/MAR), Observatorio del Estrecho (Consejería de Medio Ambiente, Junta de Andalucía) and CTM2008-06421/MAR. DM was supported by a JaeDOC contract (X0SC000087) of the Spanish Science and Technology Council (CSIC). The authors thank two anonymous reviewers for their assistance in evaluating this paper.

[21] The Editor thanks two anonymous reviewers for their assistance in evaluating this paper.

References

Arnone, R. A., D. A. Weisenburg, and K. D. Saunders (1990), The origin and characteristics of the Algerian current, *J. Geophys. Res.*, *95*(C2), 1587–1598, doi:10.1029/JC095iC02p01587.

Baldacci, A., G. Corsini, R. Grasso, G. Manzella, J. T. Allen, P. Cipollini, T. H. Guymer, and H. M. Snaith (2001), A study of the Alborán sea

mesoscale system by means of empirical orthogonal function decomposition of satellite data, *J. Mar. Syst.*, *29*, 293–311, doi:10.1016/S0924-7963(01)00021-5.

Bartolacci, D. M., and M. E. Luther (1999), Patterns of co-variability between physical and biological parameters in the Arabian Sea, *Deep Sea Res., Part II*, *46*(8–9), 1933–1964, doi:10.1016/S0967-0645(99)00049-1.

Bartual, A., D. Macías, A. Gutierrez-Rodríguez, C. M. García, and F. Echevarría (2011), Transient pulses of primary production generated by undulatory processes in the western sector of the Strait of Gibraltar, *J. Mar. Syst.*, *87*, 25–36, doi:10.1016/j.jmarsys.2011.02.021.

Björnsson, H., and S. A. Venegas (1997), A manual of EOF and SVD analysis of climate data, *C2GCR Rep. 97-1*, McGill Univ., Montreal, Quebec, Canada.

Bretherton, C. S., C. Smith, and J. M. Wallace (1992), An intercomparison of methods for finding coupled patterns in climate data, *J. Clim.*, *5*(6), 541–560, doi:10.1175/1520-0442(1992)005<0541:AIOMFF>2.0.CO;2.

Criado-Aldeanueva, F., J. Del Río Vera, and J. García-Lafuente (2008), Steric and mass-induced Mediterranean sea level trends from 14 years of altimetry data, *Global Planet. Change*, *60*(3–4), 563–575, doi:10.1016/j.gloplacha.2007.07.003.

García-Gorriz, E., and M. E. Carr (1999), The climatological annual cycle of satellite-derived phytoplankton pigments in the Alboran Sea, *Geophys. Res. Lett.*, *26*, 2985–2988, doi:10.1029/1999GL900529.

García-Lafuente, J., and J. Ruiz (2007), The Gulf of Cádiz pelagic ecosystem: A review, *Prog. Oceanogr.*, *74*(2–3), 228–251, doi:10.1016/j.pocean.2007.04.001.

García-Lafuente, J., N. Cano, M. Vargas, J. P. Rubín, and A. Hernández-Guerra (1998), Evolution of the Alborán Sea hydrographic structures during July 1993, *Deep Sea Res., Part I*, *45*(1), 39–65, doi:10.1016/S0967-0637(97)00216-1.

Isern-Fontanet, J., E. García-Ladona, and J. Font (2006), Vortices of the Mediterranean Sea: An altimetric perspective, *J. Phys. Oceanogr.*, *36*(1), 87–103, doi:10.1175/JPO2826.1.

Jordi, A., and D. P. Wang (2009), Mean dynamic topography and eddy kinetic energy in the Mediterranean Sea: Comparison between altimetry and a 1/16 degree ocean circulation model, *Ocean Modell.*, *29*(2), 137–146, doi:10.1016/j.ocemod.2009.04.001.

Jordi, A., G. Basterretxea, and S. Angles (2009), Influence of ocean circulation on phytoplankton biomass distribution in the Balearic Sea: Study based on Sea-viewing Wide Field-of-view Sensor and altimetry satellite data, *J. Geophys. Res.*, *114*, C11005, doi:10.1029/2009JC005301.

Kalnay, E., et al. (1996), The NCEP/NCAR 40-year reanalysis project, *Bull. Am. Meteorol. Soc.*, *77*, 437–471, doi:10.1175/1520-0477(1996)077<0437:TNYRP>2.0.CO;2.

Larnicol, G., N. Ayoub, and P. Y. Le Traon (2002), Major changes in Mediterranean Sea level variability from 7 years of TOPEX/Poseidon and ERS-1/2 data, *J. Mar. Syst.*, *33–34*, 63–89, doi:10.1016/S0924-7963(02)00053-2.

Le Traon, P. Y., and G. Dibarboure (1999), Mesoscale mapping capabilities of multi-satellite altimeter missions, *J. Atmos. Oceanic Technol.*, *16*, 1208–1223, doi:10.1175/1520-0426(1999)016<1208:MMCOMS>2.0.CO;2.

Le Traon, P. Y., G. Dibarboure, and N. Ducet (2001), Use of a high resolution model to analyze the mapping capabilities of multi-altimeter missions, *J. Atmos. Oceanic Technol.*, *16*, 1277–1288, doi:10.1175/1520-0426(2001)018<1277:UOAHRM>2.0.CO;2.

Macías, D., C. M. García, F. Echevarría, A. Vázquez, and M. Bruno (2006), Tidal induced variability of mixing processes on Camarinal Sill (Strait of Gibraltar): A pulsating event, *J. Mar. Syst.*, *60*, 177–192, doi:10.1016/j.jmarsys.2005.12.003.

Macías, D., et al. (2007a), Analysis of mixing and biogeochemical effects induced by tides on the Atlantic–Mediterranean flow in the Strait of Gibraltar through a physical–biological coupled model, *Prog. Oceanogr.*, *74*(2–3), 252–272, doi:10.1016/j.pocean.2007.04.006.

Macías, D., G. Navarro, F. Echevarría, C. M. García, and J. L. Cueto (2007b), Phytoplankton distribution in the north-western Alboran Sea and meteorological forcing: a remote sensing study, *J. Mar. Res.*, *65*(4), 523–543, doi:10.1357/002224007782689085.

Macías, D., M. Bruno, F. Echevarría, A. Vázquez, and C. M. García (2008), Meteorologically-induced mesoscale variability of the North-western Alborán Sea (southern Spain) and related biological patterns, *Estuarine Coastal Shelf Sci.*, *78*(2), 250–266, doi:10.1016/j.ecss.2007.12.008.

Macías, D., R. Somavilla, I. González-Gordillo, and F. Echevarría (2010), Physical control of zooplankton distribution at the Strait of Gibraltar during an episode of internal wave generation, *Mar. Ecol. Prog. Ser.*, *408*, 79–95, doi:10.3354/meps08566.

Millot, C. (1999), Circulation in the western Mediterranean Sea, *J. Mar. Syst.*, *20*, 423–442, doi:10.1016/S0924-7963(98)00078-5.

Navarro, G., and J. Ruiz (2006), Spatial and temporal variability of phytoplankton in the Gulf of Cádiz through remote sensing images, *Deep Sea Res., Part II*, *53*(11–13), 1241–1260, doi:10.1016/j.dsr2.2006.04.014.

Parada, M., and M. Canton (1998), Sea surface temperature variability in Alborán sea from satellite data, *Int. J. Remote Sens.*, *19*, 2439–2450, doi:10.1080/014311698214541.

Pascual, A., M. I. Pujol, G. Larnicol, P. Y. Le Traon, and M. H. Río (2007), Mesoscale mapping capabilities of multisatellite altimeter missions: First results with real data in the Mediterranean Sea, *J. Mar. Syst.*, *65*, 190–211, doi:10.1016/j.jmarsys.2004.12.004.

Prohaska, J. (1976), A technique for analyzing the linear relationships between two meteorological fields, *Mon. Weather Rev.*, *104*(11), 1345–1353, doi:10.1175/1520-0493(1976)104<1345:ATFATL>2.0.CO;2.

Snaith, H. M., S. G. Alderson, J. T. Allen, and J. H. Guymer (2003), Monitoring the eastern Alborán Sea using combined altimetry and in situ data, *Philos. Trans. R. Soc. A*, *361*, 65–70, doi:10.1098/rsta.2002.1109.

Vázquez, A., M. Bruno, A. Izquierdo, and D. Macías (2008), The effect of meteorologically forced subinertial flows on internal waves generation at the main sill of the Strait of Gibraltar, *Deep Sea Res., Part I*, *55*(10), 1277–1283, doi:10.1016/j.dsr.2008.05.008.

Vázquez, A., S. Flecha, M. Bruno, D. Macías, and G. Navarro (2009), Internal waves and short-scale distribution patterns of chlorophyll in the Strait of Gibraltar and Alborán Sea, *Geophys. Res. Lett.*, *36*, L23601, doi:10.1029/2009GL040959.

Vigo, I., D. Garcia, and B. F. Chao (2005), Change of sea level trend in the Mediterranean and Black seas, *J. Mar. Res.*, *63*(6), 1085–1100, doi:10.1357/002224005775247607.

Wallace, J. M., C. Smith, and C. S. Bretherton (1992), Singular value decomposition of sea surface temperature and 500-mb height anomalies, *J. Clim.*, *5*(6), 561–576, doi:10.1175/1520-0442(1992)005<0561:SVDOWS>2.0.CO;2.

M. Bruno, Centro Andaluz de Ciencia y Tecnología Marinas, Universidad de Cádiz, E-11510 Puerto Real, Spain.

D. Macías, G. Navarro, and J. Ruiz, Departamento de Ecología y Gestión Costera, Instituto de Ciencias Marinas de Andalucía, CSIC, E-11510 Puerto Real, Spain. (gabriel.navarro@icman.csic.es)

Á. Vázquez, Departamento de Física Aplicada, Universidad de Cádiz, E-11510 Puerto Real, Spain.